





## PAPER

[View Article Online](#)  
[View Journal](#) | [View Issue](#)Cite this: *Nanoscale Adv.*, 2023, 5, 2553

## Enhanced and stabilized photoluminescence of perovskite cesium lead bromide nanocubes through ordered assemblies†

Moeka Sasaki, Shota Hashimoto, Yoshiki Iso,  Yuya Oaki,  Tetsuhiko Isobe   
and Hiroaki Imai \*

This work clarified the effects of self-assembly of perovskite cesium lead bromide (CsPbBr<sub>3</sub>) nanocubes (NCs) covered with didodecylmethyl ammonium bromide (DDAB) on photoluminescence (PL) properties. Although the PL intensity of isolated NCs was weakened in the solid state even under inert conditions, the quantum yield of PL (PLQY) and the photostability of DDAB-covered NCs were drastically improved by the formation of two-dimensional (2D) ordered arrays on a substrate. The PLQY of the 2D arrays increased to ca. 60% by initial excitation illumination at 468 nm and was maintained for over 4000 h. The improved PL properties are attributable to the fixation of the surface ligand around the NCs in the specific ordered arrays.

Received 7th November 2022  
Accepted 31st March 2023

DOI: 10.1039/d2na00784c

[rsc.li/nanoscale-advances](https://rsc.li/nanoscale-advances)

## Introduction

Perovskite CsPbX<sub>3</sub> (X: Cl, Br, and I) nanoparticles attract much attention as fluorescent materials due to their excellent photoluminescence (PL) characteristics, such as tunable wavelength, narrow peak width, high absolute quantum yields of PL (PLQYs), and short lifetimes.<sup>1–4</sup> However, the PL stability of CsPbX<sub>3</sub> against light illumination, heating, humidity, and polar solvents should be improved for practical applications.<sup>5–10</sup> Nanocubes (NCs) of CsPbX<sub>3</sub> are usually synthesized by the hot-injection method.<sup>1</sup> Oleic acid (OA) and oleylamine (OLA) are used as surface ligands that cover the nanograins in liquid media. The PL performance of CsPbX<sub>3</sub> NCs is degraded with desorption of surface ligands.<sup>6,11</sup> The stabilization of CsPbX<sub>3</sub> NCs was reported by core/shell structuring,<sup>12,13</sup> hybridization with polymers,<sup>14,15</sup> cation exchange,<sup>16,17</sup> and surface passivation.<sup>18,19</sup> The original surface ligands were replaced by didodecylmethyl ammonium bromide (DDAB), which binds tightly to the ionic surface of CsPbX<sub>3</sub> for the stabilization of

PL.<sup>20–23</sup> However, the effective photostability of CsPbX<sub>3</sub> NCs has not been achieved in solid states under several days of excitation illumination. In general, the PL stability of phosphors is extremely important for practical use, and it is essential to study the degradation behavior of phosphors under long-term light irradiation. However, there are no studies regarding the degradation behavior of CsPbBr<sub>3</sub> under light irradiation for several thousand hours. For example, the PL intensity of CsPbBr<sub>3</sub> with DDAB ligand exchange in resin was reported to decrease to 70% of the initial value after blue light irradiation for 50 h.<sup>21</sup> In this study, we demonstrated the stable PL performance of CsPbBr<sub>3</sub> under long-term light irradiation of more than 4000 h.

The self-assembly of rectangular nanoblocks, such as NCs and nanocuboids, has been regarded as a fascinating bottom-up approach because single-crystal-like superstructures called mesocrystals are easily obtained by the oriented aggregation of specific crystal faces.<sup>24–31</sup> A wide variety of ordered superstructures are fabricated from various kinds of NCs.<sup>25,32–37</sup> Specific electrical, electrochemical, photonic, and mechanical properties were found to originate from the ordered structures.<sup>38–41</sup> Thus, nanometer-scale brickwork using NCs is regarded as a fundamental technique for fabricating elaborate micro- and nanostructures for exploring novel functions. In our previous work, the controlled fabrication of two-dimensional (2D) and three-dimensional (3D) arrangements of NCs and nanocuboids was demonstrated using evaporation-driven self-assembly.<sup>32,33</sup> Binary arrangements of 2D arrays are attracting attention for the enhancement of specific functions, including magnetic properties originating from large areas of heterogeneous junctions.<sup>37</sup> Since perovskite nanoparticles commonly have a cubic shape, the ordered arrays of CsPbX<sub>3</sub> NCs are easily produced

Department of Applied Chemistry, Faculty of Science and Technology, Keio University, 3-14-1 Hiyoshi, Kohoku-ku, Yokohama 223-8522, Japan. E-mail: [hiroaki@applc.keio.ac.jp](mailto:hiroaki@applc.keio.ac.jp)

† Electronic supplementary information (ESI) available: Schematic illustrations of preparation methods for various arrays of CsPbBr<sub>3</sub> NCs using an organic medium (Fig. S1); detailed conditions for the PL measurement (Fig. S2); TEM images, SAED patterns, size distribution, and appearance in a toluene dispersion of the as-synthesized NCs (Fig. S3); FT-IR spectra of CsPbBr<sub>3</sub> NCs (Fig. S4); schematic illustration of ordered 2D arrays of NCs covered with ligands (Fig. S5); Tauc plots calculated from the UV-visible absorption spectra (Fig. S6); the variation of the NC arrays under illumination (Fig. S7); schematic illustrations for the structural difference between the large and small 2D arrays and isolated NCs (Fig. S8). See DOI: <https://doi.org/10.1039/d2na00784c>

through self-assembly processes. PL properties were reported to be influenced by the 3D assembly of CsPbBr<sub>3</sub> NCs.<sup>29,31</sup> However, the influence of the ordered assembly on CsPbBr<sub>3</sub> NCs has not been studied sufficiently with regard to the PLQY and its stability.

In this paper, we clarified the effect of various assembled structures of CsPbBr<sub>3</sub> NCs covered with DDAB on PL properties. We successfully produced 2D ordered arrays of NCs on a silica glass substrate using several kinds of evaporation-driven assembly processes. The PL properties of NCs in 2D lattices were investigated by comparing them with isolated NCs. Here, the PLQY and photostability of CsPbBr<sub>3</sub> NCs were found to be strongly influenced by the ordered assembly on a substrate. The PL properties of CsPbBr<sub>3</sub> NCs are discussed based on the ligand stability in the ordered arrays. The PLQY is also important for the performance of a light emitting diode (LED).<sup>20,22</sup> Our findings in the present work are important for practical applications and the development of perovskite phosphors.

## Experimental procedures

### Preparation of CsPbBr<sub>3</sub> NCs and ligand exchange

Perovskite NCs were prepared according to a previous article.<sup>1</sup> As starting materials, we used Cs<sub>2</sub>CO<sub>3</sub> (99.99%, Mitsuwa Pure Chemical) and PbBr<sub>2</sub> (99%, Mitsuwa Pure Chemical) without further purification. A mixture of 1-octadecene (40.0 cm<sup>3</sup>) and OA (2.5 cm<sup>3</sup>) containing Cs<sub>2</sub>CO<sub>3</sub> (2.50 mmol) was vacuum-dried for 1 h at 120 °C and then heated to 150 °C under Ar until the powder was completely dissolved. The precursor solution was preheated at 100 °C before injection. A mixture of 1-octadecene (5.0 cm<sup>3</sup>) and PbBr<sub>2</sub> (0.188 mmol) was vacuum-dried for 1 h at 120 °C and then purged with Ar. OLA (0.50 cm<sup>3</sup>) and OA (0.50 cm<sup>3</sup>) were added to the mixture, which was then heated to 165 °C. We injected a preheated Cs precursor rapidly into the mixture. The resultant solution was then cooled in an ice-water bath. Solid powder was aggregated by adding *tert*-butyl alcohol (25.0 cm<sup>3</sup>) and collected by centrifugation. The resultant powders were redispersed in toluene.

The ligand exchange was performed according to a previous article.<sup>20</sup> We added OA (0.10 cm<sup>3</sup>) and 0.05 M DDAB (0.20 cm<sup>3</sup>) to a CsPbBr<sub>3</sub> NC dispersion (1.0 cm<sup>3</sup>) with a concentration of 1.87 g dm<sup>-3</sup>. Solid powder was aggregated by adding ethyl acetate (1.0 cm<sup>3</sup>) and collected by centrifugation. The ligand-exchanged CsPbBr<sub>3</sub> NCs were redispersed in toluene.

### Preparation of various CsPbBr<sub>3</sub> NC arrays

DDAB-covered CsPbBr<sub>3</sub> NCs were dispersed in an organic medium (toluene : hexane = 1 : 1 (v/v)). Highly ordered nanocube layers were formed through evaporation-driven self-assembly on a silicon substrate.<sup>31,32,34</sup> We washed silica glass substrates (7 × 16 mm) with acetone by ultrasonication for 30 min and then placed them into a 0.5 cm<sup>3</sup> organic medium containing CsPbBr<sub>3</sub> NCs in a glass vial (Fig. S1a in the ESI†). The dispersion spread on the glass substrate after immersion. The nanocube assemblies were then deposited on the substrate by the evaporation of the liquid medium (Fig. S1a in the ESI†). For

the formation of ordered monolayers, the particle concentration was adjusted to 12.7 × 10<sup>-1</sup> g dm<sup>-3</sup>. Monolayers of NCs were also prepared by a conventional spin-coating method (Fig. S1b in the ESI†). Isolated NCs were deposited on a colloidal film that was placed on a silica glass substrate through the evaporation of the liquid medium after casting a drop of the dispersion (Fig. S1c in the ESI†).

### Blue LED irradiation of the NC arrays

Irradiation was performed according to a previous study.<sup>44</sup> The NCs on the substrate were covered with a silica glass plate with ultraviolet (UV) curing resin (Bondic BD-SKEJ) to prevent degradation due to water and oxygen in the atmosphere (Fig. S2 in the ESI†). The NC films were irradiated using a flat-panel blue LED (Nissin Electronics TE-4556). A typical procedure for the PL measurement is described in Fig. S2 in the ESI†. The luminescence wavelength and irradiance were 468 nm and 48.5 W m<sup>-2</sup>, respectively. The irradiated sample was stored in the dark. A distinct increase in temperature was not observed after LED irradiation for 24 h.

### Characterization

The UV-visible absorption spectra of the dispersion and film samples were measured using UV/visible/near-infrared optical absorption spectrometers (JASCO V-750 and V-570). PL spectra were measured using a fluorescence spectrometer (JASCO FP-8500). PLQYs of the dispersion and film samples were measured using an absolute quantum yield spectrometer (Hamamatsu C9920-02G). The morphology and the crystalline phase of the NCs were monitored using transmission electron microscopy (TEM, FEI Tecnai G<sup>2</sup>), scanning electron microscopy (SEM, JEOL JSM-7100), X-ray diffractometry (XRD, Bruker D8 Advance and Bruker D8 Discover), and Fourier-transform infrared spectroscopy (FT-IR, JASCO 4200ST).

## Results and discussion

### Preparation of CsPbBr<sub>3</sub> NCs and ligand exchange

We prepared CsPbBr<sub>3</sub> NCs by the hot-injection method and then exchanged the ligands around the NCs from OA and OLA with DDAB. Fig. 1 and S3 in the ESI† show TEM images, selected-area electron diffraction (SAED) patterns, size distribution, and appearance in a toluene dispersion of ligand-exchanged (DDAB-covered) and as-synthesized NCs. The SAED patterns (Fig. 1b and S3 in the ESI†) indicate the presence of cubic CsPbBr<sub>3</sub> regardless of the ligand exchange. The average side length of NCs was estimated to be 8.6 ± 1.9 nm and 7.3 ± 1.2 nm for the as-synthesized and DDAB-covered NCs, respectively (Fig. 1a and S3 in the ESI†). The NCs were miniaturized with a slight dissolution through the ligand-exchanging process. We confirmed the presence of DDAB based on FT-IR spectra of NCs before and after ligand exchange (Fig. S4 in the ESI†). Intense PL at around 520 nm was observed by excitation at 470 nm (Fig. 1c). A slight shift in the PL peak with the ligand exchange is ascribed to a decrease in the size of NCs (Fig. S3 in the ESI†). The PLQY increased to *ca.* 80% from *ca.*



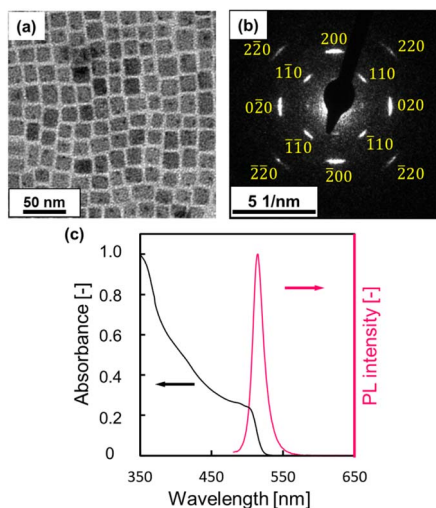


Fig. 1 (a) Schematic TEM image, (b) SAED pattern, and (c) optical properties of DDAB-covered CsPbBr<sub>3</sub> NCs.

30% by the ligand exchange. In a previous study, the PLQY was improved by reducing the cesium, lead, and bromide defects in CsPbBr<sub>3</sub>.<sup>23,30</sup> The increase in the PLQY was ascribed to a decrease in the number of bromide vacancies or low-coordinate lead ions through surface passivation by DDAB (Fig. S5 in the ESI<sup>†</sup>), which adsorbs to the surface more rigidly than the original ligands, such as OA and OLA.<sup>20</sup> Therefore, the improvement in PLQY suggests a decrease in the trap density.

### Assembly of CsPbBr<sub>3</sub> NCs

As shown in Fig. 2 and S6 in the ESI,<sup>†</sup> we successfully produced various arrangements of CsPbBr<sub>3</sub> NCs using several methods. Detailed conditions for the arrangements are described in the ESI.<sup>†</sup> Here we obtained two kinds of 2D arrays (monolayered NCs) of CsPbBr<sub>3</sub> NCs on a silica glass substrate.

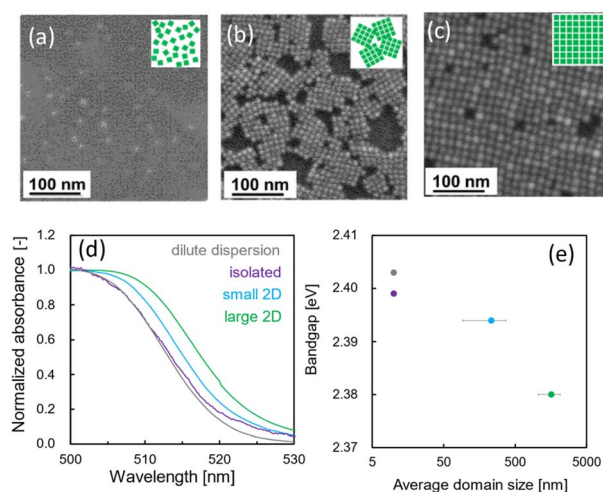


Fig. 2 (a–c) SEM images with schematic illustrations, (d) UV absorption edges, and (e)  $E_g$  as a function of the domain size in NC arrays; (a) isolated NCs, (b) small 2D arrays, and (c) large 2D arrays.

Moreover, isolated NCs were prepared on a collodion film. The ordered domain scale of 2D arrays was *ca.* 100 nm in the small 2D array and *ca.* 500 nm in the large 2D array. Ordered assemblies of NCs covered with ligands are basically formed *via* oriented self-assembly with lateral capillary force at the liquid–air interface. Random aggregation through direct attachment of the NCs is prevented by the surface ligands (Fig. S5 in the ESI<sup>†</sup>).

The absorption edge shifted to a higher wavelength as the size of the ordered domains increased. The bandgap ( $E_g$ ) of CsPbBr<sub>3</sub> NCs in various states was determined from a Tauc plot calculated from the UV-visible absorption spectra (Fig. S6 in the ESI<sup>†</sup>). This indicates bandgap shrinkage through the formation of a mini-band with strong interaction between the NCs, as reported in a previous study.<sup>29</sup>

### Photoactivation and photostability of CsPbBr<sub>3</sub> NCs

Fig. 3a–d show the appearance and the PL spectra of the large 2D and isolated NCs before and after blue light illumination at 450 nm. Since the absolute PL intensity was proportional to the occupancy of NCs on the substrate, the emission of the large 2D array was larger than that of the small 2D array and the isolated NCs. Interestingly, the PL intensities of the isolated NCs on a substrate were weak and decreased to *ca.* 60% of the initial value after 120 h of irradiation (Fig. 3c). The PL was not recognized by visual evaluation after 3600 h (Fig. 3a). On the other hand, the PL intensity of the small and large 2D arrays steeply increased with initial illumination for 72 h (Fig. 3d). The time

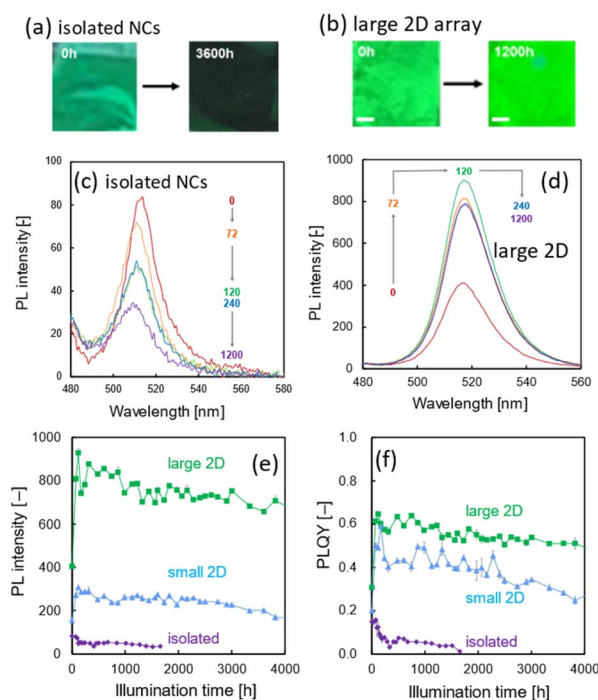


Fig. 3 (a and b) Changes in PL and (c and d) PL spectra of isolated NCs and large 2D arrays of CsPbBr<sub>3</sub> NCs under illumination at 450 nm; (e and f) time courses of PL intensity and the PLQY of small and large 2D arrays and isolated NCs under illumination at 450 nm.

courses of the PL intensity and the PLQY of the small and large 2D arrays and isolated NCs under illumination are shown in Fig. 3e and f. The initial and final values of PLQY for the isolated NCs were *ca.* 20% and 10%, respectively. Although the initial values of PLQY of the 2D arrays were *ca.* 20%, they were boosted to 50–60% and maintained for over 4000 h. Thus, the ordered arrays of DDAB-covered NCs enhanced the photoactivation and suppressed the degradation of the PL intensity.

The enhancement of the PLQY for the large 2D array was higher than that for the small 2D arrays. This suggests that the regularity of the arrangement influences photoactivation and photostabilization. We confirmed the repeatability of the assembly-enhanced PL intensity using another set of 2D arrays and isolated NCs on the substrate (Fig. S7 in the ESI†).

The essence of photostability is the rigid adsorption of ligand molecules on the crystal surface. Fig. 4 shows schematic illustrations of the photodegradation and photoactivation mechanisms for isolated NCs and 2D arrays. The ligands would gradually desorb from the isolated NCs, resulting in luminescence quenching because of non-radiative relaxation through the surface trap levels. The PL intensity of CsPbBr<sub>3</sub> NCs in resin decreased under light illumination.<sup>21</sup> In contrast, silica coating was found to induce effective photostability,<sup>42,43</sup> because the desorption of the ligands on NCs is suppressed by the covered silica. Our results indicate that the desorption of the ligands on NCs is suppressed by the neighboring NCs on the substrate. Moreover, the photoactivation was remarkable for the 2D arrays. This means that the initial state of the ligands in the arrays is disordered. The initial illumination arranges the ligands between NCs in the ordered arrays. The higher regularity contributes to the higher stability of the ligand arrangements.

The structure difference between the large and small 2D arrays and isolated NCs is explained in Fig. S8 in the ESI.† We compared the ratio of the total area attached to other NCs to the total surface area of NCs. All the faces of the isolated NCs are not attached to other NCs. In the small and large 2D arrays, about 90% and 99% of the faces of NCs are attached to other NCs respectively. The higher ratio of the total surface area in contact with other NCs improves the PLQY and the photostability, because the surface ligands between two faces are not easily desorbed.

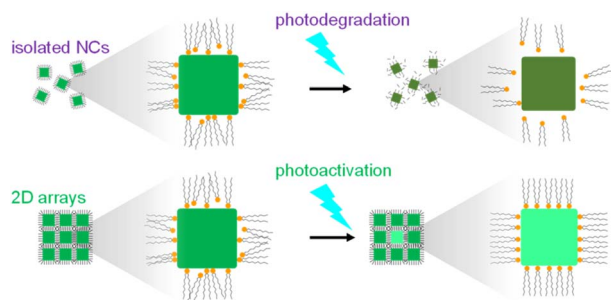


Fig. 4 Schematic illustrations of the photodegradation and photoactivation mechanisms for isolated NCs and 2D arrays.

## Conclusion

We found that the self-assembly of perovskite cesium lead bromide (CsPbBr<sub>3</sub>) nanocubes (NCs) enhances and stabilizes photoluminescence (PL) properties. The CsPbBr<sub>3</sub> NCs covered with didodecyldimethyl ammonium bromide in 2D ordered arrays are activated and stabilized by blue illumination. The PLQY of the 2D arrays increased to *ca.* 60% from *ca.* 30% by initial excitation illumination at 468 nm and was maintained for over 4000 h. The enhancement effect of the ordered structures is important for practical applications and the development of perovskite phosphors.

## Conflicts of interest

The authors declare no competing financial interests.

## Acknowledgements

This work was supported by JSPS KAKENHI grant number JP21H01627.

## References

- 1 L. Protesescu, S. Yakunin, M. I. Bodnarchuk, F. Krieg, R. Caputo, C. H. Hendon, R. X. Yang, A. Walsh and M. V. Kovalenko, *Nano Lett.*, 2015, **15**, 3692–3696.
- 2 G. Nedelcu, L. Protesescu, S. Yakunin, M. I. Bodnarchuk, M. J. Grotevent and M. V. Kovalenko, *Nano Lett.*, 2015, **15**, 5635–5640.
- 3 A. Swarnkar, R. Chulliyil, V. K. Ravi, M. Irfanullah, A. Chowdhury and A. Nag, *Angew. Chem., Int. Ed.*, 2015, **54**, 15424–15428.
- 4 Q. A. Akkerman, V. D'Innocenzo, S. Accornero, A. Scarpellini, A. Petrozza, M. Prato and L. Manna, *J. Am. Chem. Soc.*, 2015, **137**, 10276–10281.
- 5 S. Huang, Z. Li, B. Wang, N. Zhu, C. Zhang, L. Kong, Q. Zhang, A. Shan and L. Li, *ACS Appl. Mater. Interfaces*, 2017, **9**, 7249–7258.
- 6 J. Liu, K. Song, Y. Shin, X. Liu, J. Chen, K. X. Yao, J. Pan, C. Yang, J. Yin, L.-J. Xu, H. Yang, A. M. El-Zohry, B. Xin, S. Mitra, M. N. Hedhili, I. S. Roqan, O. F. Mohammed, Y. Han and O. M. Bakr, *Chem. Mater.*, 2019, **31**, 6642–6649.
- 7 Y. Wei, Z. Cheng and J. Lin, *Chem. Soc. Rev.*, 2019, **48**, 310–350.
- 8 X. Yuan, X. Hou, J. Li, C. Qu, W. Zhang, J. Zhao and H. Li, *Phys. Chem. Chem. Phys.*, 2017, **19**, 8934–8940.
- 9 D. Di Girolamo, M. I. Dar, D. Dini, L. Gontrani, R. Caminiti, A. Mattoni, M. Graetzel and S. Meloni, *J. Mater. Chem. A*, 2019, **7**, 12292–12302.
- 10 Y. Kim, E. Yassitepe, O. Voznyy, R. Comin, G. Walters, X. Gong, P. Kanjanaboos, A. F. Nogueira and E. H. Sargent, *ACS Appl. Mater. Interfaces*, 2015, **7**, 25007–25013.
- 11 J. De Roo, M. Ibáñez, P. Geiregat, G. Nedelcu, W. Walravens, J. Maes, J. C. Martins, I. Van Driessche, M. V. Kovalenko and Z. Hens, *ACS Nano*, 2016, **10**, 2071–2081.



- 12 Q. Zhong, M. Cao, H. Hu, D. Yang, M. Chen, P. Li, L. Wu and Q. Zhang, *ACS Nano*, 2018, **12**, 8579–8587.
- 13 Z. Li, E. Hofman, J. Li, A. H. Davis, C. Tung, L. Wu and W. Zheng, *Adv. Funct. Mater.*, 2018, **28**, 1704288.
- 14 Y. Xin, H. Zhao and J. Zhang, *ACS Appl. Mater. Interfaces*, 2018, **10**, 4971–4980.
- 15 Y. Cai, L. Wang, T. Zhou, P. Zheng, Y. Li and R.-J. Xie, *Nanoscale*, 2018, **10**, 21441–21450.
- 16 W. van der Stam, J. J. Geuchies, T. Altantzis, K. H. W. van den Bos, J. D. Meeldijk, S. Van Aert, S. Bals, D. Vanmaekelbergh and C. de Mello Donega, *J. Am. Chem. Soc.*, 2017, **139**, 4087–4097.
- 17 S. Zou, Y. Liu, J. Li, C. Liu, R. Feng, F. Jiang, Y. Li, J. Song, H. Zeng, M. Hong and X. Chen, *J. Am. Chem. Soc.*, 2017, **139**, 11443–11450.
- 18 L. Xu, J. Li, B. Cai, J. Song, F. Zhang, T. Fang and H. Zeng, *Nat. Commun.*, 2020, **11**, 3902.
- 19 Y. Cao, W. Zhu, L. Li, Z. Zhang, Z. Chen, Y. Lin and J.-J. Zhu, *Nanoscale*, 2020, **12**, 7321–7329.
- 20 J. H. Park, A. Lee, J. C. Yu, Y. S. Nam, Y. Choi, J. Park and M. H. Song, *ACS Appl. Mater. Interfaces*, 2019, **11**, 8428–8435.
- 21 W. Zheng, Z. Li, C. Zhang, B. Wang, Q. Zhang, Q. Wan, L. Kong and L. Li, *Nano Res.*, 2019, **12**, 1461–1465.
- 22 J. Pan, L. N. Quan, Y. Zhao, W. Peng, B. Murali, S. P. Sarmah, M. Yuan, L. Sinatra, N. M. Alyami, J. Liu, E. Yassitepe, Z. Yang, O. Voznyy, R. Comin, M. N. Hedhili, O. F. Mohammed, Z. H. Lu, D. H. Kim, E. H. Sargent and O. M. Bakr, *Adv. Mater.*, 2016, **28**, 8718–8725.
- 23 M. Imran, P. Ijaz, L. Goldoni, D. Maggioni, U. Petralanda, M. Prato, G. Almeida, I. Infante and L. Manna, *ACS Energy Lett.*, 2019, **4**, 819–824.
- 24 T. Wang, X. Wang, D. LaMontagne, Z. Wang, Z. Wang and Y. C. Cao, *J. Am. Chem. Soc.*, 2012, **134**, 18225–18228.
- 25 K. Tsukiyama, M. Takasaki, N. Kitamura, Y. Idemoto, Y. Oaki, M. Osada and H. Imai, *Nanoscale*, 2019, **11**, 4523–4530.
- 26 K. Mimura, *J. Ceram. Soc. Jpn.*, 2016, **124**, 848–854.
- 27 S. Disch, E. Wetterskog, R. P. Hermann, G. Salazar-Alvarez, P. Busch, T. Brückel, L. Bergström and S. Kamali, *Nano Lett.*, 2011, **11**, 1651–1656.
- 28 J. Brunner, I. A. Baburin, S. Sturm, K. Kvashnina, A. Rossberg, T. Pietsch, S. Andreev, E. Sturm née Rosseeva and H. Cölfen, *Adv. Mater. Interfaces*, 2017, **4**, 1600431.
- 29 Y. Tong, E.-P. Yao, A. Manzi, E. Bladt, K. Wang, M. Döblinger, S. Bals, P. Müller-Buschbaum, A. S. Urban, L. Polavarapu and J. Feldmann, *Adv. Mater.*, 2018, **30**, 1801117.
- 30 G. Rainò, M. A. Becker, M. I. Bodnarchuk, R. F. Mahrt, M. V. Kovalenko and T. Stöferle, *Nature*, 2018, **563**, 671–675.
- 31 D. Baranov, S. Toso, M. Imran and L. Manna, *J. Phys. Chem. Lett.*, 2019, **10**, 655–660.
- 32 Y. Nakagawa, H. Kageyama, Y. Oaki and H. Imai, *J. Am. Chem. Soc.*, 2014, **136**, 3716–3719.
- 33 Y. Nakagawa, R. Matsumoto, H. Kageyama, Y. Oaki and H. Imai, *Nanoscale*, 2018, **10**, 12957–12962.
- 34 R. Matsumoto, Y. Nakagawa, H. Kageyama, Y. Oaki and H. Imai, *CrystEngComm*, 2016, **18**, 6138–6142.
- 35 R. Matsumoto, M. Takasaki, K. Tsukiyama, Y. Oaki and H. Imai, *Inorg. Chem.*, 2018, **57**, 11655–11661.
- 36 H. Imai, R. Matsumoto, M. Takasaki, K. Tsukiyama, K. Sawano and Y. Nakagawa, *CrystEngComm*, 2019, **21**, 6905–6914.
- 37 K. Sawano, K. Tsukiyama, M. Shimizu, M. Takasaki, Y. Oaki, T. Yamamoto, Y. Einaga, C. Jenewein, H. Cölfen, H. Kaiju, T. Sato and H. Imai, *Nanoscale*, 2020, **12**, 7792–7796.
- 38 S. Deng, V. Tjoa, H. M. Fan, H. R. Tan, D. C. Sayle, M. Olivo, S. Mhaisalkar, J. Wei and C. H. Sow, *J. Am. Chem. Soc.*, 2012, **134**, 4905–4917.
- 39 M. Jehannin, A. Rao and H. Cölfen, *J. Am. Chem. Soc.*, 2019, **141**, 10120–10136.
- 40 J. Cai and L. Qi, *Sci. China: Chem.*, 2012, **55**, 2318–2326.
- 41 J. Ihli, A. N. Kulak and F. C. Meldrum, *Chem. Commun.*, 2013, **49**, 3134.
- 42 H. Hu, L. Wu, Y. Tan, Q. Zhong, M. Chen, Y. Qiu, D. Yang, B. Sun, Q. Zhang and Y. Yin, *J. Am. Chem. Soc.*, 2018, **140**, 406–412.
- 43 Q. Zhang, B. Wang, W. Zheng, L. Kong, Q. Wan, C. Zhang, Z. Li, X. Cao, M. Liu and L. Li, *Nat. Commun.*, 2020, **11**, 31.
- 44 K. Kidokoro, Y. Iso and T. Isobe, *J. Mater. Chem. C*, 2019, **7**, 8546–8550.

